

Supporting Information

Triplet Exciton Diffusion and Quenching in Matrix-Free Solid Photon Upconversion Films

*Steponas Raišys,[†] Ona Adomėnienė,[†] Povilas Adomėnas[†] Alexander Rudnick[§], Anna Köhler[§]
and Karolis Kazlauskas^{*†}*

[†] Institute of Photonics and Nanotechnology, Vilnius University, Saulėtekio av. 3, LT-10257
Vilnius, Lithuania.

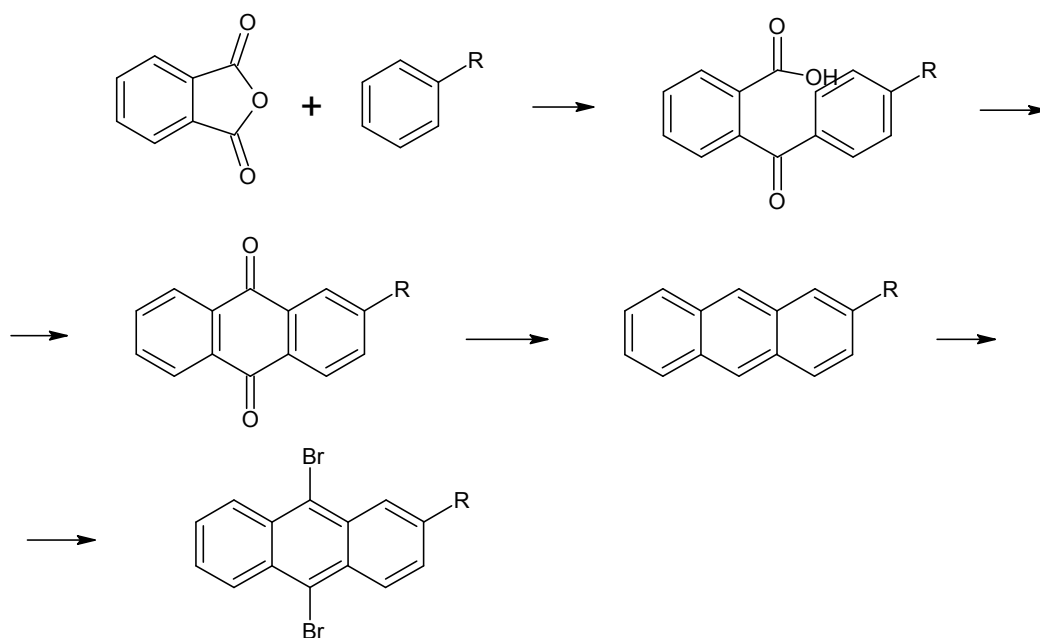
[§] Soft Matter Optoelectronics, Department of Physics & Bayreuth Institute of
Macromolecular Reserach (BIMF), University of Bayreuth, Bayreuth 95440, Germany

**E-mail: karolis.kazlauskas@ff.vu.lt*

SYNTHESIS AND IDENTIFICATION

Solvents were purified using standard procedures. Reactions were carried out under dry argon atmosphere using magnetic stirring. All reactions and purity of the synthesized compounds were monitored by gas chromatography using Agilent Technologies 7890A GC System with triple axis detector 5975C inert XL MSD and Agilent Technologies 6890N Network GC System, and TLC using Silica gel 60 F254 aluminum plates (Merck). Synthesized compounds were purified by preparative column chromatography using silica gel Kieselgel 60 0.06-0.2 mm. Proton and carbon nuclear magnetic resonance (^1H and ^{13}C NMR) spectra were recorded on Varian Unity Inova (300 MHz) or Bruker ASCEND (400 MHz) spectrometer in chloroform- d_3 or benzene- d_6 , using residual solvent signal as an internal standard.

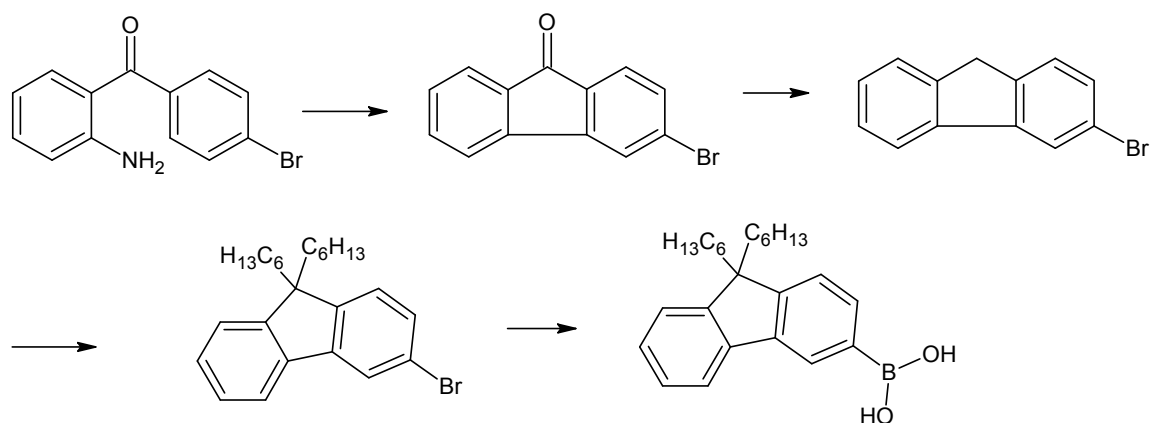
The intermediate 9,10-dibromo-2-substituted anthracenes were obtained by the usual sequence of transformations, starting from phthalic anhydride and biphenyl or toluene:



where R = C_6H_5 - or CH_3 - groups.

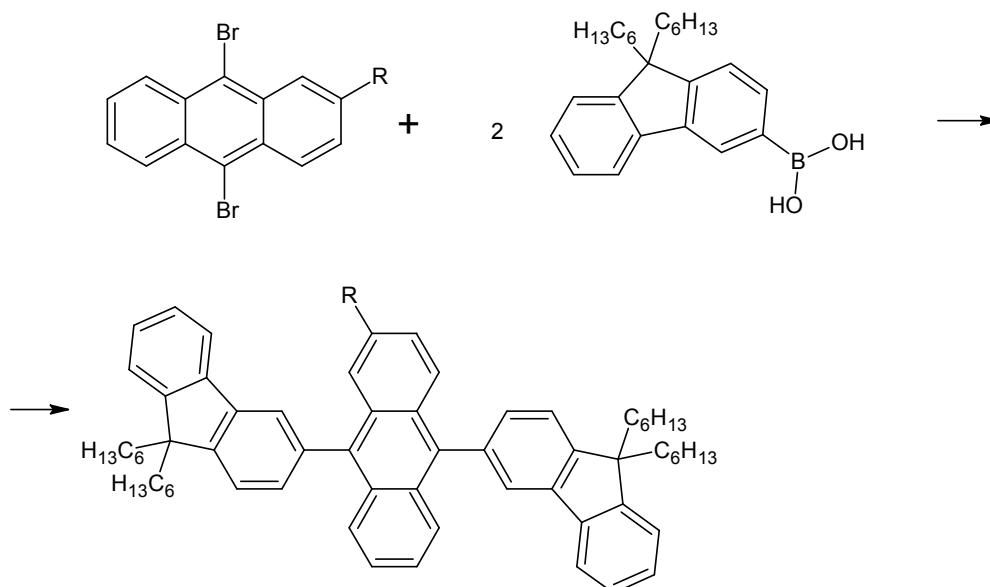
Scheme S1. Synthesis of intermediate 9,10-dibromo-2-substituted anthracenes.

The fluorene part was obtained by the following transformations:



Scheme S2. Synthesis of intermediate dihexyl-fluorenes.

Finally, the target compounds were obtained by a cross-coupling reaction between anthracene and fluorene components:



where R = CH₃ (resulting in target compound **BFA-Me**) or
R = C₆H₅ (resulting in target compound **BFA-Ph**).

Scheme S3. Synthesis of the target compounds **BFA-Me** and **BFA-Ph**.

(4-Phenylbenzoyl)-2-benzenecarboxylic acid. 2 L glass bulb equipped with mechanical stirrer, thermometer and reflux condenser was placed in an ice bath, charged with 1.2 L dichloroethane and cooled down to 0–5 °C. While stirring, 139 g (0.9 mol) of biphenyl, 120 g (0.9 mol) of aluminum trichloride and 133 g (0.9 mol) of phthalic anhydride was added at such a rate that the temperature was maintained within 0–5 °C. After introducing all the reagents, the mixture was stirred still for 0.5h. Then the ice bath was changed to a water bath and heated up to +40 °C. 120 g (0.9 mol) of aluminum chloride was added portionwise while keeping the

temperature within 40-45 °C. The released hydrogen chloride through reflux condenser was absorbed in sodium hydroxide solution. After the introduction of aluminum chloride, the reaction mixture was stirred at 40-45 °C for 2 h more and then poured into an ice – 0.2L hydrochloric acid mixture. The solid product was filtered off, washed three times with water and dried at 100 °C. 253 g of 2-(4-phenylbenzoyl)benzenecarboxylic acid was obtained, which was used in the next reaction step without an additional purification.

2-Phenylanthraquinone. 2L glass bulb was charged with 800 g of polyphosphoric acid and heated up to 160 °C. Then in 20 min 253 g (0.836 mol) of 2-(4-phenylbenzoyl)benzenecarboxylic acid was added and stirred still for 4.5 h at 160-166 °C. Later the mixture was cooled down to +140 °C and poured into 5L of hot water; then it left over night to cool down. After filtering the mixture, the solid was placed into 10% aqueous potassium hydroxide solution. The mixture was boiled for 0.5h and filtered; the remaining solid was washed by water and filtered again. The solid was extracted using 1.3L of toluene, concentrated and the remainder was distilled under vacuum, b.p. 220-275 °C /1 Torr. 126 g (0.443 mol) of 2-phenylanthraquinone was obtained at a yield of 53%; m.p. 162-163 °C.

2-Phenylanthracene was obtained by reduction of the above 2-phenylanthraquinone by aluminum chloride-lithium aluminum hydride, according to Ref.¹.

9,10-Dibromo-2-phenylanthracene. 6L round glass bulb was charged with 1.5L of dichloromethane, cooled down in an ice bath to 8-10 °C, which was followed by the addition of 76 g (0.30 mol) of 2-phenylanthracene. Into the formed suspension a solution of bromine (86 g; 0.60 mol) in 250 ml of dichloromethane was added dropwise. After the addition of bromine solution, which took 2 hours, the mixture was stirred at room temperature for 40 min. Then 0.5L of water and 15 g of sodium sulfite were added and the mixture was filtered through glass filter. The layers were separated; the organic layer was washed by water, separated and concentrated. The solid once again was washed by water, dried at room temperature and then crystallized from 1400 ml of toluene. Yield 104 g (84%), dark yellow crystalline material. M.p. 176-178 °C.

9,10-Dibromo-2-methylantracene was prepared in a similar way from 2-methylantracene with a yield of 82%. The product was obtained as dark yellow crystalline powder, m.p. 142-143 °C. The 2-methylantracene was obtained by an acylation of toluene with phthalic anhydride, cyclization by 2-(4-methylbenzoyl)benzenecarboxylic acid and reduction of the obtained 2-methylantraquinone.²

3-Bromo-9H-fluoren-9-one was obtained according to Ref.³, by diazotization of 2-amino-4'-bromobenzophenone.

3-Bromo-9H-fluorene was obtained according to Ref.⁴, by a reduction of 3-bromo-9H-fluoren-9-one with hydrazine hydrate in diethylene glycol. Yield 82%; m.p. 90-91 °C.

3-Bromo-9,9-di-n-hexyl-9H-fluorene. 1L round glass bulb was charged with 150 ml of dry tetrahydrofuran (THF) under argon flow, then 42 g (0.37 mol) of potassium tert-butoxide was added. A solution of 36.7 g (0.15 mol) of 3-bromo-9H-fluorene in 150 ml of THF was added dropwise without cooling; the temperature raised to +54 °C. The mixture was stirred at room temperature for 1h, then 6 g (0.37 mol) of 1-bromohexane was introduced dropwise during 0.5h. The mixture was stirred at 50 °C for another 1h. Then the mixture was poured into water, acidified by aqueous hydrogen chloride and extracted with dichloromethane (2 x 150ml). The organic layer was separated, washed by water and evaporated. The remainder was crystallized from 2-propanol (1:3) at -30 °C. 40 g light off-white solid was obtained at a yield of 80%; m.p. 42-43 °C.

3-(9,9'-Dihexyl-9H-fluorenyl)boronic acid. 3-Bromo-9,9'-dihexyl-9H-fluorene (26 g; 62 mmol) was dissolved in 200 ml of anhydrous THF, the solution was cooled down to -70 °C. Then 26 ml of 25% butyllithium hexane solution (70 mmol) was added dropwise and stirred at this temperature for 1 h. Trimethylborate (10.4 g; 100 mmol) solution in 30 ml of THF was added dropwise to a resulting mixture and left to warm up to room temperature. 6 ml of water, and later, 40 ml of 10% sulphuric acid was added to the stirred mixture. The boronic acid was extracted by using toluene (2 x 100 ml), evaporated and purified by flash-chromatography (silicagel, eluent hexane-ethyl acetate, 2:1). 13 g of 3-(9,9-dihexyl-9H-fluorenyl)boronic acid was obtained at a yield of 55%; m.p. 150 °C.

2-Methyl-9,10-bis(9,9-dihexyl-9H-fluoren-3-yl)anthracene (BFA-Me). A glass bulb in an argon flow was charged with 20 ml of toluene, 0.53 g (1.5 mmol) of 2-methyl-9,10-dibromoanthracene, 1.21 g (3.2 mmol) of 3-(9,9-dihexyl-9H-fluorenyl)boronic acid, 70 mg (0.1 mmol) of bis(triphenylphosphino)palladium dichloride and 55 mg (0.2 mmol) of triphenylphosphine. The mixture was stirred and heated to 80 °C. At this temperature a solution of 1.08 g (10 mmol) of sodium carbonate in 7 ml of water was added dropwise. Then the mixture was heated at reflux for 6h under argon flow. The organic layer was separated, cooled down to room temperature and the solid product was filtered off. The toluene was evaporated from filtrate; both solid fractions were combined and purified by column chromatography on silica gel utilizing solvent hexane-toluene (10:1). Later, the solvent was thoroughly evaporated. 1.01 g of light yellow crystalline product was obtained at a yield of 73%; m.p. 140-142°C.

¹H NMR (CDCl₃), δ: 0.80-0.87 (m, 12H), 1.14-1.25 (m, 32H), 1.59 (s, 3H), 2.08-2.16 (m, 8H), 7.05-8.09 (m, 22H).

¹³C NMR (CDCl₃), δ: 14.12, 21.69, 22.63, 23.95, 29.81, 31.60, 40.52, 55.19, 118.73, 119.88, 119.94, 122.64, 122.77, 123.02, 123.43, 123.63, 124.34, 124.60, 124.91, 125.22, 126.39, 126.54, 126.79, 126.90, 127.01, 127.11, 127.20, 127.40, 127.59, 127.84, 128.09, 128.78, 129.63, 130.11, 130.30, 130.40, 131.56, 131.67, 134.55, 136.42, 137.29, 137.59, 137.70, 140.42, 140.61, 140.85, 140.89, 140.96, 141.04, 141.30, 149.91, 149.97, 150.70, 150.94, 151.11.

2-Phenyl-9,10-bis(9,9-dihexyl-9H-fluoren-3-yl)anthracene (BFA-Ph). A glass bulb in an argon flow was charged with 50 ml of toluene, 0.62 g (1.5 mmol) of 2-phenyl-9,10-

dibromoanthracene, 1.32 g (3.5 mmol) of 3-(9,9-dihexyl-9H-fluorenyl)boronic acid, 70 mg (0.1 mmol) of bis(triphenylphosphino)palladium dichloride and 55 mg (0.2 mmol) of triphenylphosphine. The mixture was stirred and heated to 80 °C. At this temperature a solution of 1.08 g (10 mmol) sodium carbonate in 7 ml of water was added dropwise and the mixture was heated at reflux for 6h under argon flow. The organic layer was separated, cooled down to room temperature and the solid product was filtered off. The toluene was evaporated from filtrate; both solid fractions were combined and purified by column chromatography on silica gel utilizing solvent hexane-toluene (10:1). Later, the solvent was thoroughly evaporated. 1.01 g colorless crystalline product was obtained at a yield of 73%; m.p. 130 °C.

^1H NMR (CDCl_3), δ : 0.82-0.91 (m, 12H), 1.15-1.28 (m, 32H), 2.13-2.17 (t, $J=8$ Hz, 8H), 7.26-7.98 (m, 26H).

^{13}C NMR (101 MHz, CDCl_3) δ 151.28, 151.22, 150.26, 150.15, 141.58, 141.50, 141.49, 141.16, 141.13, 141.06, 138.02, 137.62, 137.55, 137.49, 137.14, 130.66, 130.59, 130.40, 130.30, 130.27, 130.24, 129.49, 128.91, 127.96, 127.41, 127.35, 127.33, 127.30, 127.23, 126.97, 125.32, 125.23, 125.07, 124.85, 123.18, 123.09, 123.01, 122.99, 122.96, 122.94, 122.78, 122.75, 120.08, 120.02, 55.32, 40.75, 40.61, 31.86, 31.74, 30.01, 29.96, 29.94, 24.10, 24.05, 22.88, 22.78, 22.77, 14.23.

The MS spectrum of compounds were obtained using MALDI-TOF instrument. The molecular mass obtained is consistent with the proposed structure.

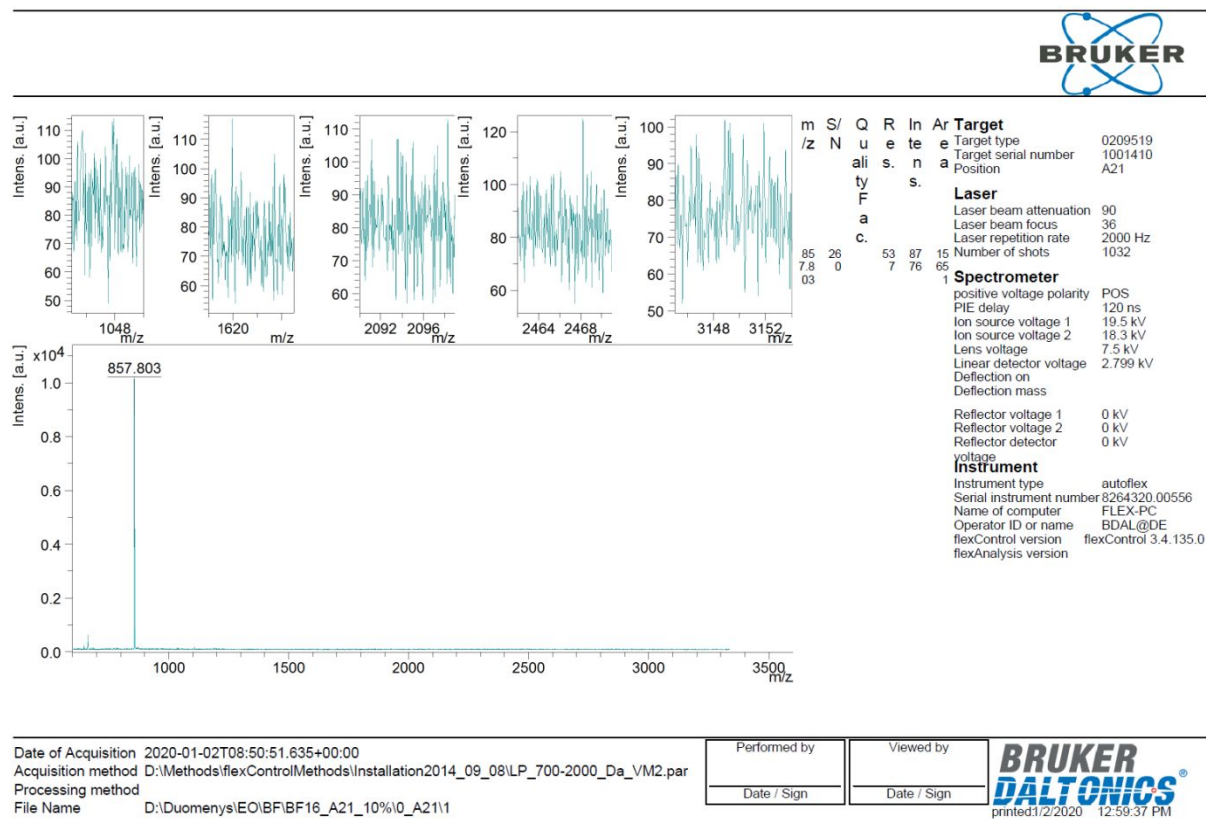
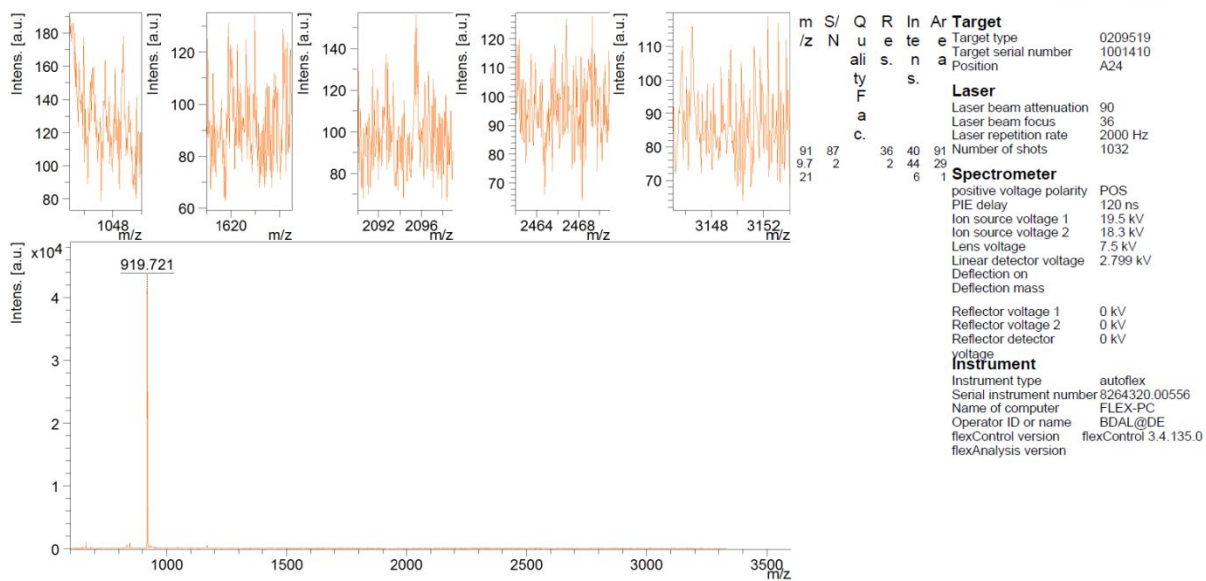


Figure S1. MALDI-TOF spectrum of BFA-Me.



Date of Acquisition 2020-01-02T08:51:23.518+00:00
 Acquisition method D:\Methods\flexControl\Methods\Installation2014_09_08\LP_700-2000_Da_VM2.par
 Processing method
 File Name D:\Duomenys\EO\BFBF17_A24_10%\0_A24\1

Performed by	Viewed by
Date / Sign	Date / Sign

BRUKER DALTONICS
 printed:1/2/2020 8:56:47 AM

Figure S2. MALDI-TOF spectrum of **BFA-Ph**.

THERMAL PROPERTIES

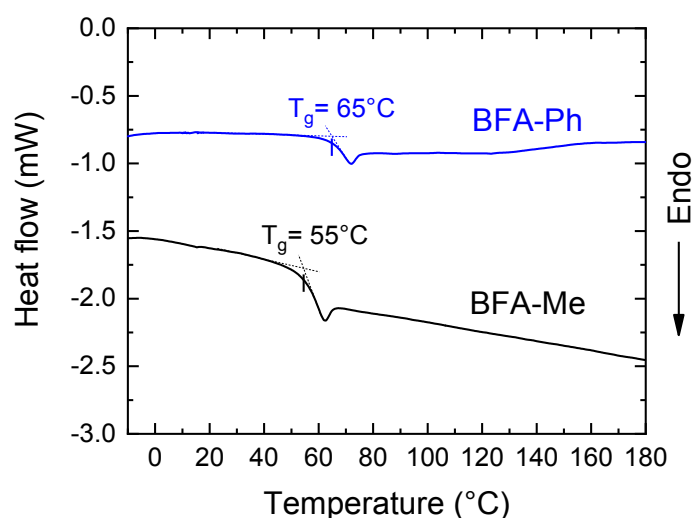


Figure S3. DSC 2nd heating scans of BFA compounds recorded at a heating rate of $10^\circ\text{C min}^{-1}$ under nitrogen flow. Glass transition (T_g) temperatures, indicated.

NANOSCALE THERMAL ANALYSIS OF BFA AND PtOEP-DOPED BFA UPCONVERTING FILMS

The technique employs specialized AFM probe, which is brought into contact with the sample surface.⁵ Upon heating the end of the tip, its deflection is measured. Heating causes sample to expand, thereby increasing tip deflection. At a transition temperature, the material typically softens allowing the probe to penetrate the sample, thus decreasing the deflection of the tip. The change in the slope of deflection signal is an indication of a thermal transition. The reference measurement of PMMA film with known T_g (Figure S6) ensured reliable estimation of T_g temperatures.⁶

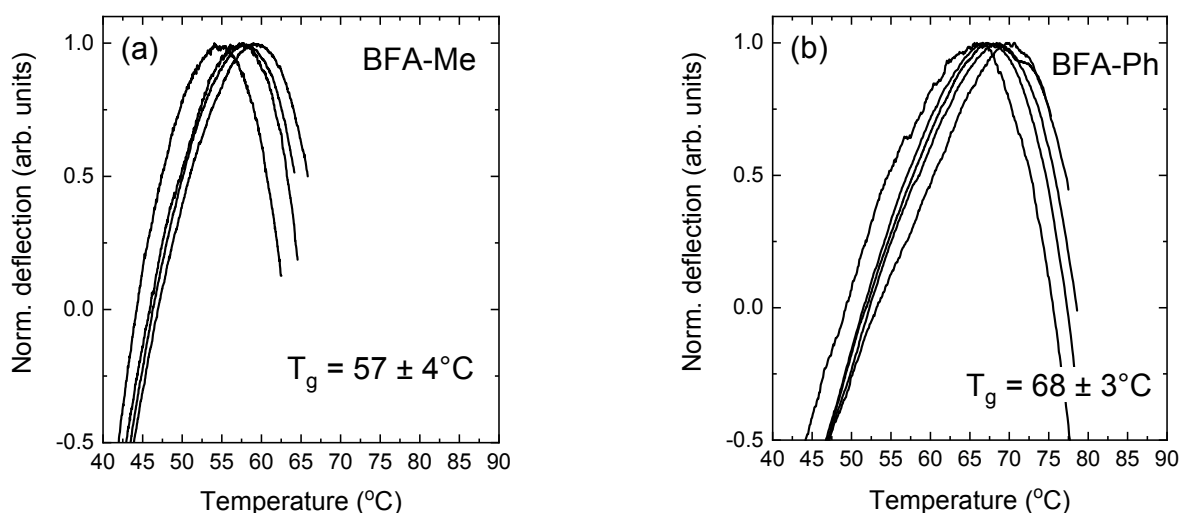


Figure S4. Normalized tip deflection vs temperature for (a) BFA-Me and (b) BFA-Ph films. Each curve corresponds to a different spot analyzed. Heating rate, 5°C per min . T_g temperatures, indicated.

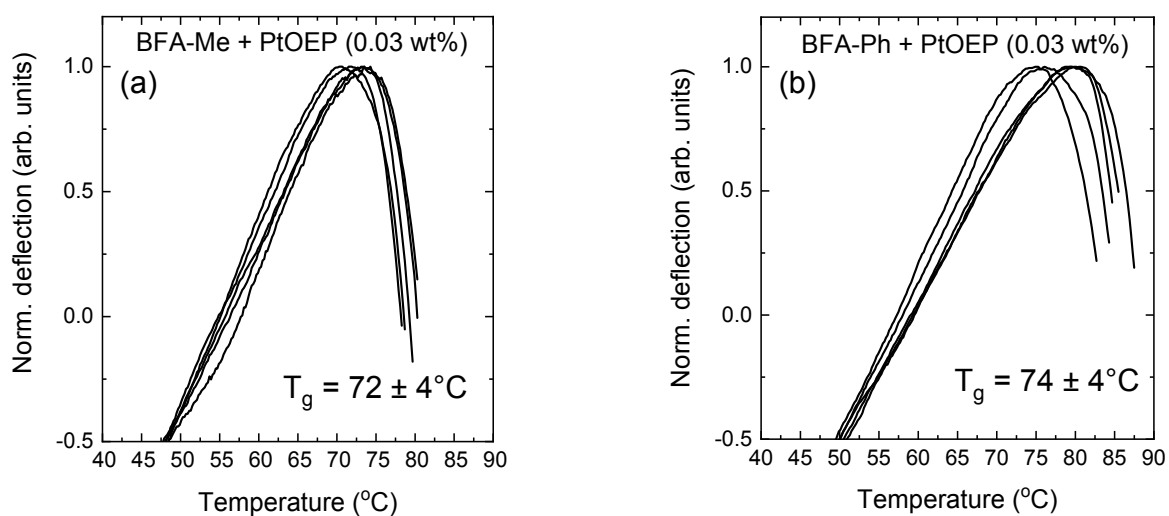


Figure S5. Normalized deflection vs temperature for (a) BFA-Me and (b) BFA-Ph films doped with 0.03 wt% of PtOEP sensitizer. Each curve corresponds to a different spot analyzed. Heating rate, 5°C per min. T_g temperatures, indicated.

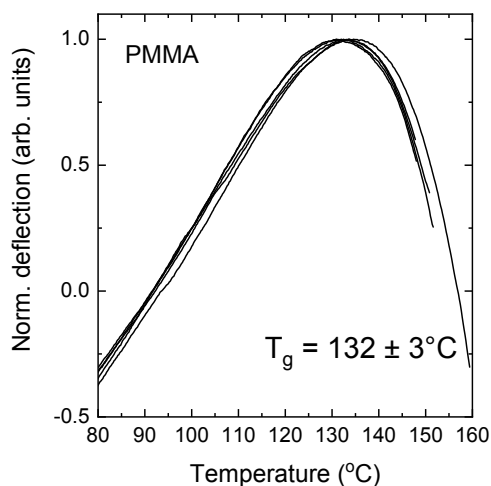


Figure S6. Normalized deflection vs temperature of the reference PMMA film. Each line corresponds to a different spot analyzed. Heating rate, 10°C per min. T_g temperature, indicated.

OPTICAL PROPERTIES

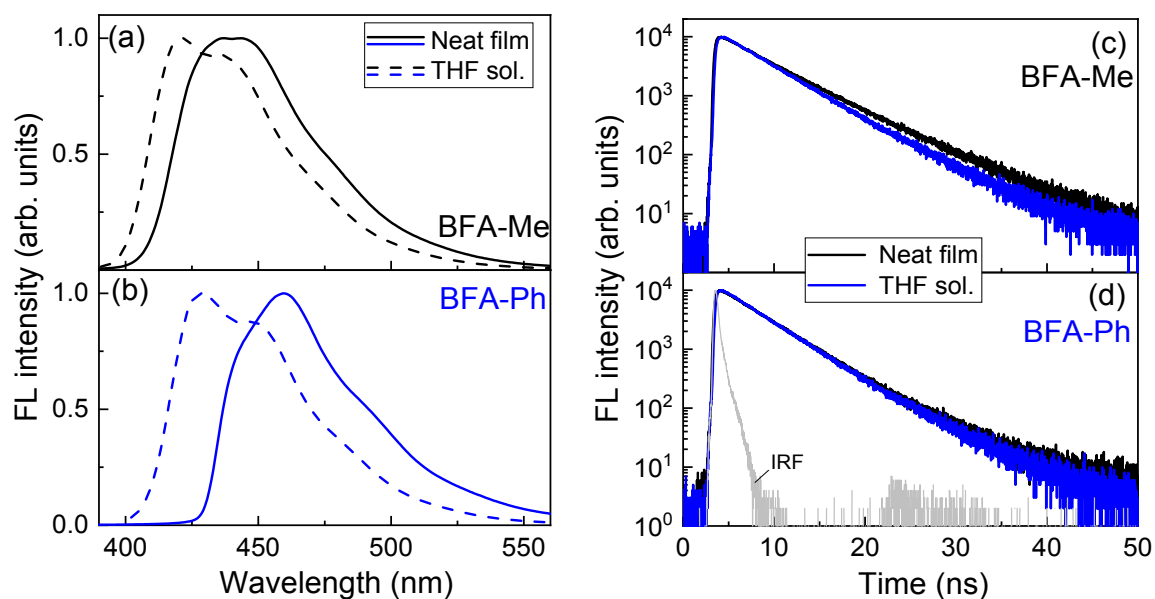


Figure S7. (a), (b) Fluorescence spectra and (c), (d) transients of BFA-Me and BFA-Ph measured in dilute THF solutions ($C = 10^{-5}\text{M}$) and neat films. Excitation wavelength – 370 nm. IRF – instrument response function.

The fluorescence spectra of dilute THF solutions are peaking at 422 and 429 nm for BFA-Me and BFA-Ph compounds, respectively. The spectra are blueshifted as compared to those of the neat films by 15 nm and 30 nm. The blue shift mainly originates from the differences in environment polarity. Additionally, neat film spectra experience enhanced reabsorption effect resulting in the diminished first vibronic peak. However, the bandwidths of the solid state and solution spectra are nearly the same suggesting the minor influence of intermolecular interactions. This is also supported by Φ_{FL} and fluorescence transient measurements. Φ_{LF} were determined to be 69% and 50% for BFA-Me and BFA-Ph, respectively, in dilute THF solutions, which are similar to the values found for the neat films, i.e. 71% and 53% for BFA-Me and BFA-Ph, respectively. Measurement accuracy of Φ_{FL} is $\pm 5\%$. Moreover, fluorescence transients of both compounds (which were described by a single exponential decay profile) are found to be also similar in solution and solid-state. The estimated lifetimes were 4.7 and 4.4 ns in THF solutions and 5.4 and 4.5 ns in the neat films for BFA-Me and BFA-Ph, respectively.

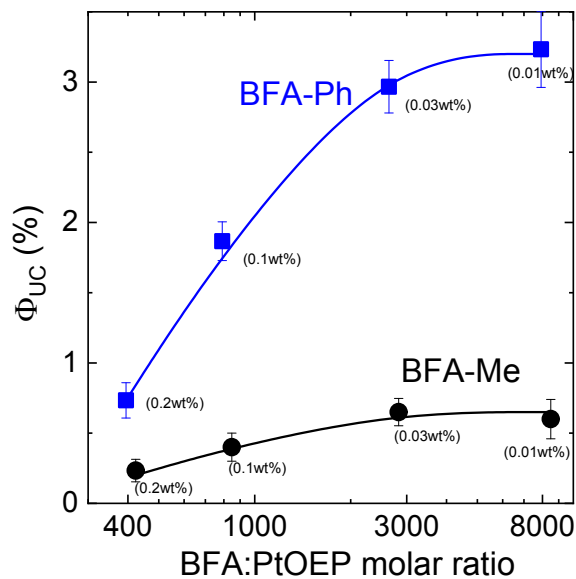


Figure S8. TTA-UC quantum yield as a function of acceptor/sensitizer (BFA:PtOEP) molar ratio for BFA-Me and BFA-Ph films. Lines are guide to the eye. Concentrations by weight percentage is indicated in parentheses. Density of BFA films was set to 1.2 g/cm³ in molar ratio calculations.

Although decreasing PtOEP concentration from 0.03 wt% further down to 0.01 wt% slightly enhanced Φ_{UC} , this significantly reduced PtOEP absorption and subsequently drastically weakened UC intensity. To make UC measurements, particularly UC transient measurements, sufficiently reliable, PtOEP concentration in the studied UC films was fixed at 0.03 wt%.

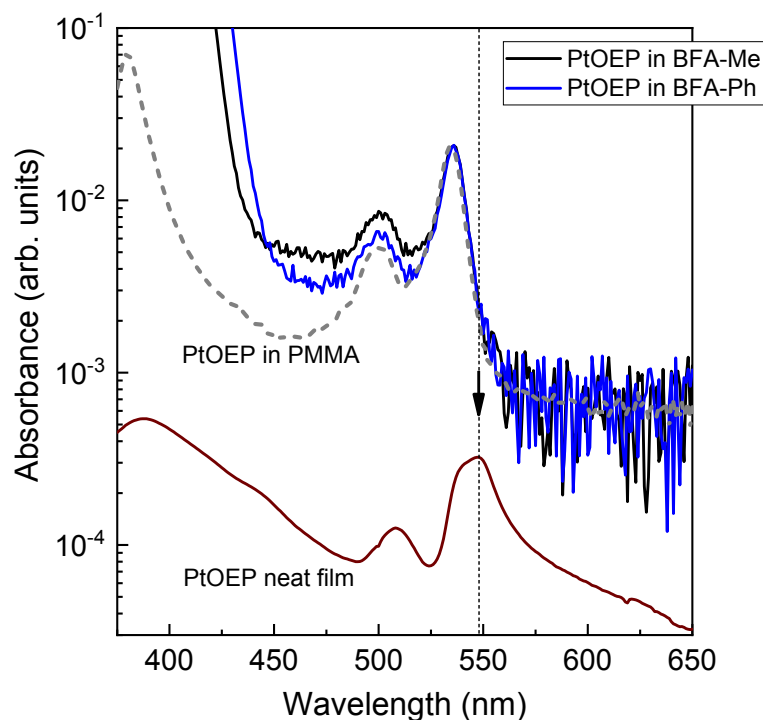


Figure S9. Absorption spectra of PtOEP sensitizer dispersed in BFA-Me, BFA-Ph and PMMA films at 0.03 wt% doping concentration. Absorption spectrum of PtOEP neat film (vertically shifted for clarity) with an arrow indicating the aggregate band is shown for comparison.

Due to a very low sensitizer PtOEP concentration in BFA films (0.03wt%), and consequently, the small number of PtOEP aggregates, the later cannot be discerned in the absorption spectra of BFA/PtOEP films. The figure above provides the absorption spectra of PtOEP sensitizer measured in BFA-Me, BFA-Ph and PMMA films. PtOEP concentration in all those films is the same (0.03 wt%). It has been shown previously, that PtOEP aggregation in PMMA film is absent up to 0.2 wt% of PtOEP (see Ref. 7 and Fig. S2 therein for confirmation), thus PtOEP in PMMA spectrum serves as a reference for aggregate-free absorption. On the other hand, the spectrum of neat PtOEP film dominated by aggregate absorption is also provided for comparison. If present, the distinct band due to aggregates (indicated by an arrow) should appear on the long wavelength slope of BFA/PtOEP spectra (black and blue solid lines). However, the later spectra nicely coincide with that of aggregate-free PtOEP spectrum in PMMA host (shown by the dashed gray line), indicating that the number of PtOEP aggregates is in turn very small. Importantly, this also implies that by exciting UC emission in BFA/PtOEP films via the sensitizer band @532nm, we mainly excite single molecules of the sensitizer and not aggregates.

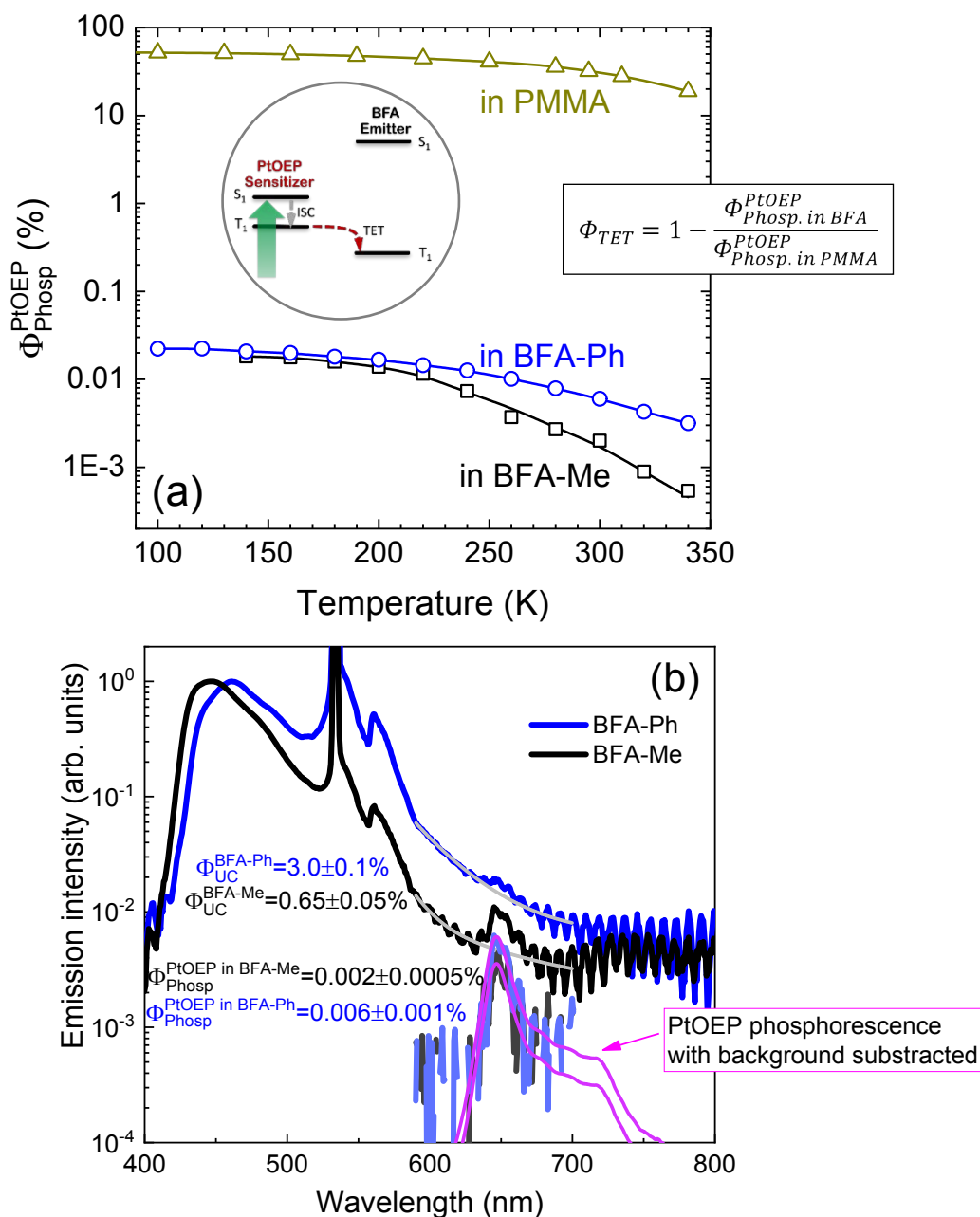


Figure S10. (a) Phosphorescence quantum yield of PtOEP in inert PMMA as well as in BFA-Me and BFA-Ph hosts as a function of temperature. Lines are guides to the eye. Inset schematically illustrates allowed triplet energy transfer from PtOEP to BFA. Φ_{Phosp}^{PtOEP} in PMMA at room temperature was determined by using an integrating sphere, and then this value ($\Phi_{Phosp}^{PtOEP} = 32\%$) was used as a reference to scale phosphorescence intensity data points measured at lower and higher temperatures. PtOEP absorption change over temperature was taken into account. (b) Room temperature Φ_{Phosp}^{PtOEP} in BFA hosts were determined by comparing spectrally integrated UC emission of the particular host (with known quantum yield, which was measured by using integrating sphere) with that of PtOEP emission (with unknown quantum yield). Similarly, room temperature Φ_{Phosp}^{PtOEP} values in each BFA host was used as a reference to scale phosphorescence intensity data points measured at lower and higher temperatures for that host.

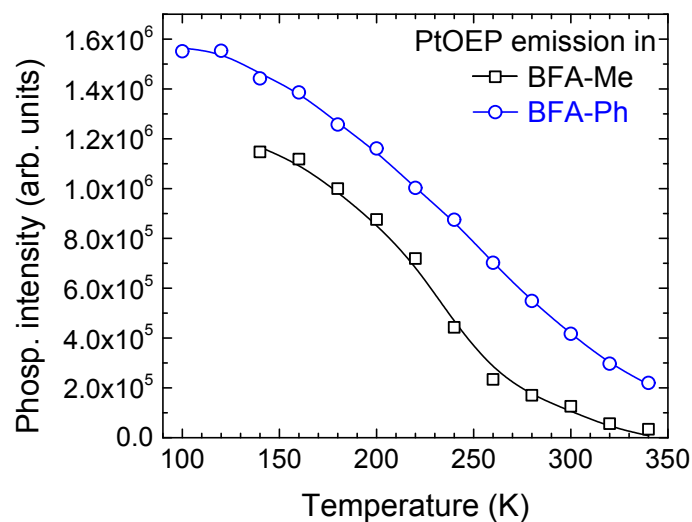


Figure S11. Phosphorescence intensity of PtOEP in BFA/PtOEP films (measured at 644 nm and at a delay of 10 μ s) as a function of temperature. Lines are guides to the eye.

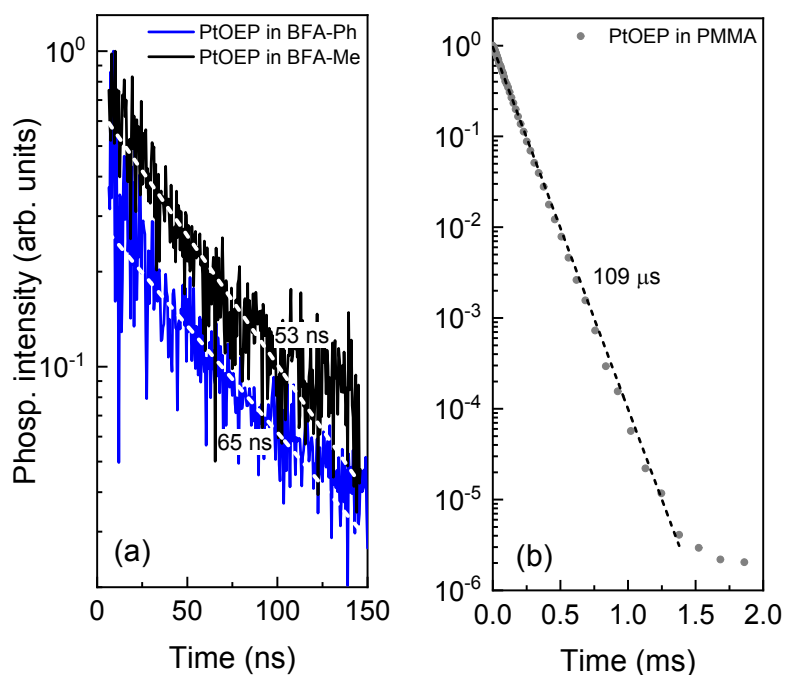


Figure S12. Phosphorescence transients of PtOEP in (a) BFA-Me and BFA-Ph and (b) PMMA films measured at 645 nm. PtOEP concentration – 0.03 wt%. Dashed lines show one exponential fits. Emission lifetimes, indicated.

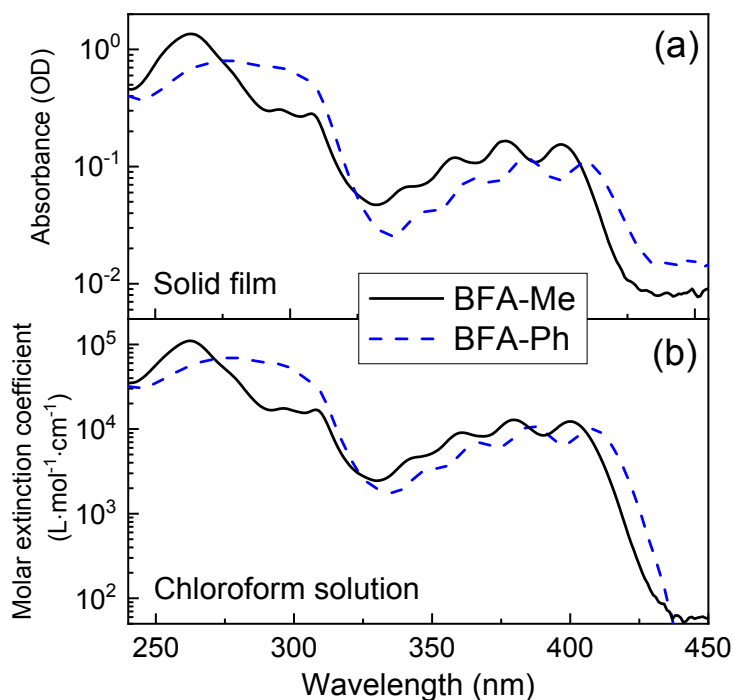


Figure S13. (a) Absorption spectra of spin-coated neat BFA films (film thickness 110 ± 1 nm) and (b) molar extinction coefficient of BFA compounds in chloroform solution ($c = 1 \cdot 10^{-5}$ M).

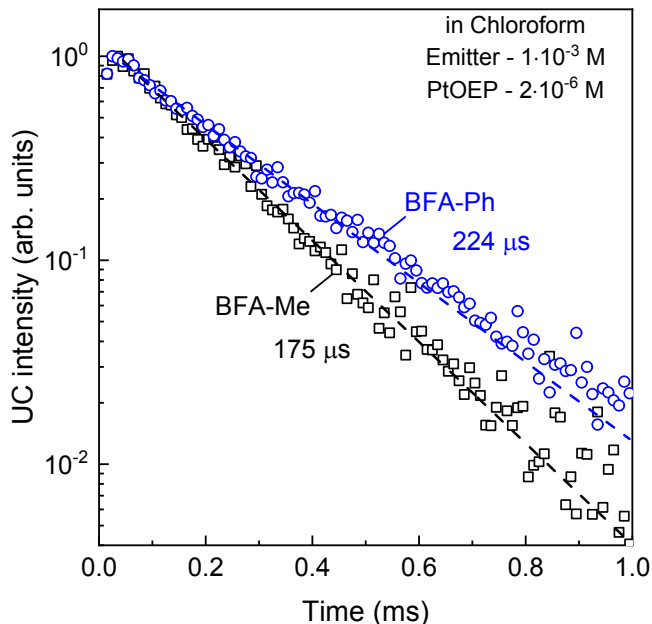


Figure S14. UC emission transients of BFA-Me/PtOEP and BFA-Ph/PtOEP in chloroform. Emitter and sensitizer concentrations were set to $1 \cdot 10^{-3}$ M and $2 \cdot 10^{-6}$ M, respectively. The transients were normalized at Time = 0 ms. Dashed lines show one exponential fits. Emission lifetimes, indicated.

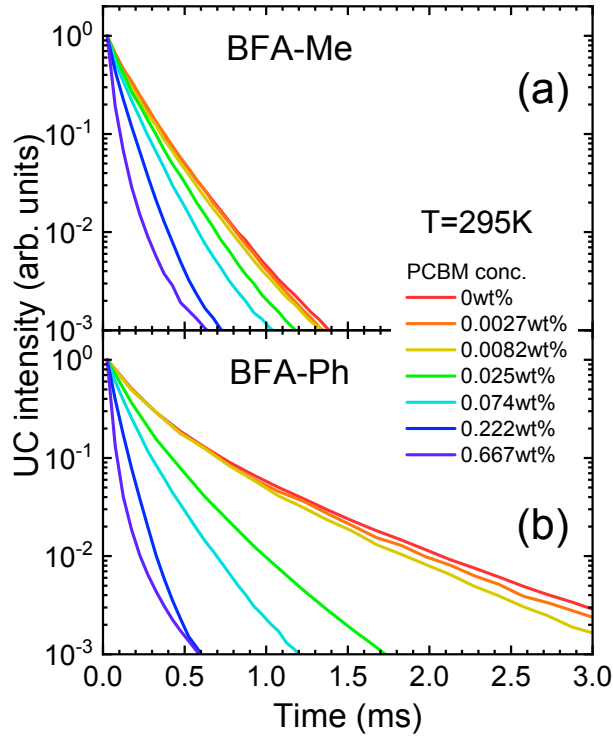


Figure S15. UC emission transients of (a) BFA-Me/PtOEP and (b) BFA-Ph/PtOEP films as a function of PCBM quencher concentration at 295 K. The transients were normalized at Time = 0 ms.

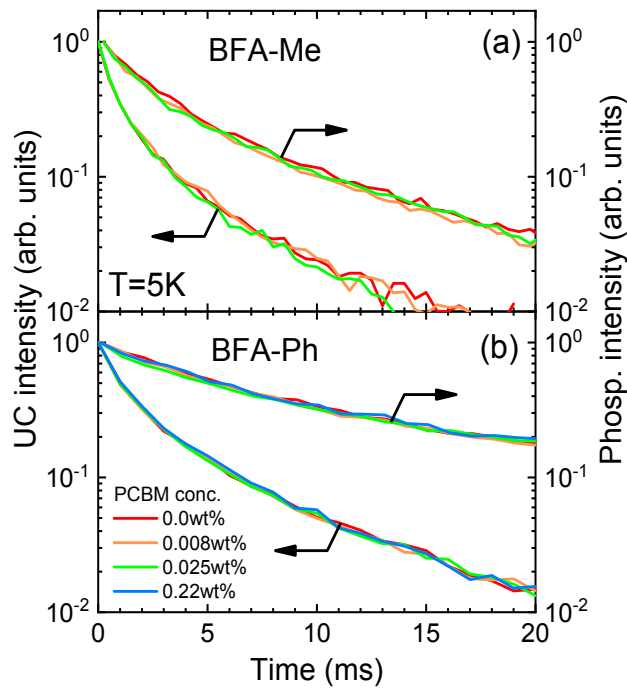


Figure S16. UC emission and phosphorescence transients of (a) BFA-Me/PtOEP and (b) BFA-Ph/PtOEP films as a function of PCBM quencher concentration at 5 K. The transients were normalized at Time = 0 ms.

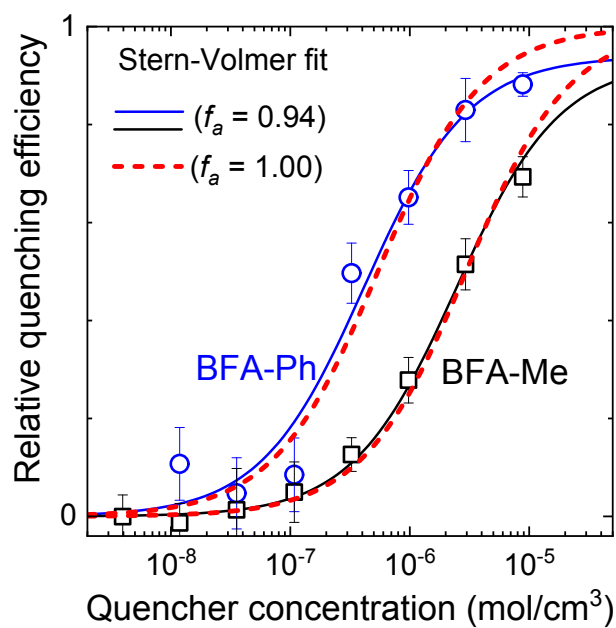


Figure S17. Relative quenching efficiency vs molar quencher concentration of BFA/PtOEP films at 295 K temperature. Solid and dashed lines show Stern-Volmer fits with $f_a = 0.94$ and $f_a = 1$, respectively.

ESTIMATION OF THE TRIPLET CONCENTRATION AT EXCITATION CONDITIONS USED IN UC TRANSIENT MEASUREMENTS

Energy density per pulse $600 \mu\text{J}/\text{cm}^2$ is a rather high excitation, since the whole energy is delivered during a very short time (pulse duration – 7 ns) compared to the millisecond lifetime of triplet excitons. Pulse repetition rate (20 Hz) doesn't play a role here, because at room temperature the triplet population completely decays during the time between the pulses (see Figure 7). Below, we provide an estimation of the triplet concentration, which essentially shows that at early decay times it is above the threshold concentration attained at I_{th} .

In a steady state regime employed to determine the threshold, the triplet concentration $[T]$ at I_{th} can be found from:

$$[T] = \frac{1}{2k_T} \cdot G = \frac{1}{2(\tau_T)^{-1}} \cdot \frac{\alpha \cdot I_{\text{th}} \cdot \Phi_{\text{TET}}}{h\nu}, \text{ where } G \text{ is triplet generation, } k_T (=1/\tau_T) - \text{triplet}$$

spontaneous relaxation rate, α - absorption coefficient, I_{th} – photon number/ cm^2 at threshold intensity, Φ_{TET} - energy transfer efficiency (=1), $h\nu$ – incident energy quanta converted to joules. Taking into account that $8 \mu\text{m}$ -thick UC films absorb only 4.5% of the incident excitation (at 532 nm), α is calculated to be $\sim 57 \text{ cm}^{-1}$. By taking τ_T from Table 1 and I_{th} from Fig. 5, we estimate triplet concentration at the threshold to be as follows $[T]_{\text{BFA-Me}} = 5.0 \cdot 10^{16} \text{ cm}^{-3}$ and $[T]_{\text{BFA-Ph}} = 6.3 \cdot 10^{15} \text{ cm}^{-3}$.

Energy density per pulse $600 \mu\text{J}/\text{cm}^2$ employed in the UC transient experiments (Figure 7) translates to $1.6 \cdot 10^{15}$ photons/ cm^2 , yielding maximum possible triplet concentration of $1.6 \cdot 10^{15} \text{ photons}/\text{cm}^2 \times 57 \text{ cm}^{-1} = 9.1 \cdot 10^{16} \text{ triplets}/\text{cm}^3$.

On the other hand, PtOEP molecular concentration at 0.03 wt% in BFA films is somewhat higher: $\frac{0.0003 \cdot \rho_{\text{BFA}} \cdot N_A}{M_{\text{PtOEP}}} = 3.0 \cdot 10^{17} \text{ molecules}/\text{cm}^3$. Here ρ_{BFA} is the film density, which for amorphous small-molecule films typically is $\approx 1.2 \text{ g}/\text{cm}^3$, M_{PtOEP} – PtOEP molar mass and N_A – Avogadro number. This means that, in fact, we have $9.1 \cdot 10^{16} \text{ triplets}/\text{cm}^3$ in BFA films. Since this concentration is higher than the threshold concentration attained at I_{th} , i.e., $[T]_{\text{BFA-Me}}$ and $[T]_{\text{BFA-Ph}}$, at early times bimolecular recombination dominates over spontaneous triplet relaxation. This is evidenced from the decay slope of -1 (Figure 7). Indeed, the slope of -1 to -1.5 in the TTA-UC transients represents a regime where triplet exciton diffusion is dispersive and γ_{TTA} is time dependent. The slope of -2 should indicate TTA dominant decay, however, in non-dispersive regime. The absence of this regime in Figure 7 suggests that during the dispersive regime, the triplet concentration already decreased below the threshold level. In later conditions, spontaneous triplet decay featuring an exponential decay profile outcompetes the bimolecular channel.

REFERENCES

- (1) Bailey, D.; Seifi, N.; Williams, V. E. Steric Effects on [4+4]-Photocycloaddition Reactions between Complementary Anthracene Derivatives. *Dyes Pigm.* **2011**, *89* (3), 313–318.
- (2) Wang, J.; Leung, L. M. Synthesis and Characterization of Highly Soluble Blue Emitting Poly(2-Vinylanthracene) with 9,10-Di(2-Naphthalenyl) and 9,10-Di(3-Quinoliny) Substituents. *Dyes Pigm.* **2013**, *99* (1), 105–115.
- (3) Bhatt, M. V. Quinone Studies—I: Evidence for a New Type of Substitution Reaction of Phenanthrene-9,10-Quinone Derivatives. *Tetrahedron* **1964**, *20* (4), 803–821.
- (4) Bancroft, K. C. C.; Bott, R. W.; Eaborn, C. 927. Aromatic Reactivity. Part XXIX. Diphenylmethane and Fluorene in Detritiation. *J. Chem. Soc.* **1964**, No. 0, 4806–4811.
- (5) Application Note 200: Correlation Between Nanoscale and Bulk Thermal Analysis <https://www.bruker.com/products/surface-and-dimensional-analysis/nanoscale-infrared-spectrometers/featured-application-notes-and-briefs/application-note-200-correlation-between-nanoscale-and-bulk-thermal-analysis.html> (accessed Sep 30, 2020).
- (6) Park, J. H.; Hwang, D. K.; Lee, J.; Im, S.; Kim, E. Studies on Poly(Methyl Methacrylate) Dielectric Layer for Field Effect Transistor: Influence of Polymer Tacticity. *Thin Solid Films* **2007**, *515* (7), 4041–4044.
- (7) Raišys, S.; Kazlauskas, K.; Juršėnas, S.; Simon, Y. C. The Role of Triplet Exciton Diffusion in Light-Upconverting Polymer Glasses. *ACS Appl. Mater. Interfaces* **2016**, *8* (24), 15732–15740.